Control of excitability to prevent the spread of pathological activity

Markus A. Dahlem, Felix M. Schneider, Eckehard Schöll

***Abstract*— Spatio-temporal excitation patterns in various neurological disorders constitute examples of excitable behaviour emerging from pathological pathways. During migraine, seizure, and stroke, an initially localized pathological state can start to spread indicating a transition from unexcitable to excitable media. We investigate this transition in the generic FitzHugh-Nagumo (FHN) system. Our goal is to define an efficient control minimizing the volume of invaded tissue. We show how to change parameters of the system so as to efficiently protect tissue surrounding a stimulus against recruitment. Furthermore, we show that wave propagation can be suppressed with a nonlocal cross coupling scheme. The area in the parameter plane where this control goal is achieved resembles a Mexican-hat-type network connectivity. This suggest that failures in synaptic transmission result in increased susceptibility of cortical tissue to pathological activity. Such a modulation of excitability becomes of crucial importance when the cortical state is close to the bifurcation of the onset of wave propagation. The clinically relevant conclusion to be drawn from this is that therapy might target network connectivity that modulates cortical tissue excitability.**

Three paradigmatic clinical manifestations of spreading pathological states motivate efforts to understand how the spread of such states arises and how it can be controlled. First, in migraine with aura seizure-like activity spreads slowly through parts of the cortex [1], [2], [3]. This is observed by symptomatic [4] and electrophysiological [5] events. Second, epileptic seizures can have a localized onset and then grow in intensity and start to spread [6], [7]. This usually leads to subsequent generalized motor involvement commonly referred to as partial seizures with secondary generalization. In some cases, however, the epileptiform activity may induce changes to subcortical structures producing clinical signs of general motor involvement that merely mimic a spread [8]. And third, during stroke a cortical region that surrounds the infarct core and that initially suffers functional injury can gradually and progressively fail and suffer irreversible structural injury in untreated patients [9], [10], [11], [12], [13], [14]. In this condition the electrophysiological changes are persistent, but there exist intermediate repetitive TWF and it was suggested that 'therapy might [...] target the intermediate forms of spreading depolarizations so as to protect the penumbra [tissue surrounding the infarct core] against recruitment into the infarct core' [15].

The phenotypical manifestation of such spreading pathological states is the phenomenon of spreading depression (SD) [16]. SD is the basis of migraine with aura. Essentially identical electrophysiological features are associated with infarct expansion, called peri-infarct depolarization (PID) [17], [18], [19]. The cascade of events that produce SD is related to seizures [20]. Despite certain differences, seizure events that begin with epileptiform discharges can either terminate in SD, facilitate the synchronization, or spread by a similar mechanism over a large area with a velocity resembling that of SD [21], [6], [22]. SD is seizure-like activity evolving as a slowly spreading non-or-all type process. It is characterized by the feedback of ion currents that change ion concentrations, which, in turn, influence the membrane potential [20], [23]. Shortly after its onset all neuronal activity is depressed, hence its name. The name is misleading, because SD can still be observed even when neuronal activity is depressed by blocking the fast transient sodium current I_{Na} [24]. SD emerges from an excitable pathway in neuronal tissue independently of the normal neuronal activity. It was therefore suggested to categorize SD and similar phenomena under the term spreading depolarizations [15].

There is ample evidence that SD belongs to the self-organization processes due to the coupling of biochemical reaction with diffusion [25], [26]. Mathematical models of SD have been suggested [27], [28], [29], [20], [23], though there is not yet consent on the mechanism. We will use

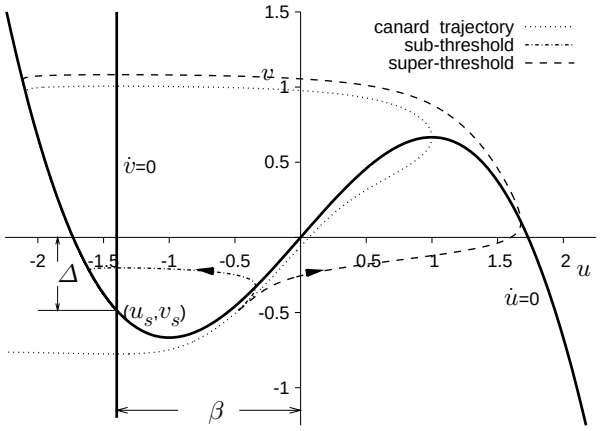

Fig. 1. The nullclines (bold) $\dot{u} = 0$ and $\dot{v} = 0$ in the phase space of the homogeneous FHN system with $\gamma = 0, \beta = 1.4$. Their intersection at (u_s, v_s) is a stable fixed point. Three trajectories are drawn for $\epsilon = 0.04$: one canard trajectory (dotted), passing through the maximum of the nullisocline $\dot{u} = 0$, and two trajectories starting at $v = v_s$ nearby but on opposite sides of the canard trajectory. They diverge sharply, producing threshold behavior: (dashed) = super-threshold and (dashed-dotted) = sub-threshold stimulation. The parameter β correlates with the threshold size, while Δ is in a certain range inversely related and therefore correlates with the excitability of the system (see text).

This work was supported by DFG in the framework of Sfb 555 and the Sachbeihilfe DA-602/1-1. We are grateful to G. Bordyugov for fruitful discussions.

Institut für Theoretische Physik, Technische Universität Berlin, Hardenbergstraße 36, D-10623 Berlin, Germany

the spatially extended FitzHugh-Nagumo (FHN) system as a generic model of neuronal excitation patterns based on reaction-diffusion. As a neuronal model, it describes generic pattern formation properties not limited to nerve impulse propagation along an axon, although it was originally derived from the Hodgkin-Huxley model of action potentials [30], [31], [32]. The FHN system describes also the spatial features of SD wave in neuronal tissue [33]. Furthermore, the transition from non-excitable to excitable media supporting traveling waves was well investigated in the FHN model [34], [35]. It was suggested that the spatio-temporal patterns in SD occur at this transition [33]. The regime in which this transition takes place is also well investigated in chemical model systems in experiment and theory, for a review see [36].

The route to spreading excitability in a generic model is provided by two independent pathways: one lowering the threshold of evoked activity, the other changing the ratio of the biochemical reaction rates, and hence the time scale ratio. The two pathways might offer new opportunities in developing optimal therapy. Consider the case that a pathological condition is caused by a shift along one path whereas therapeutic strategies are available for both pathways. Suppose both strategies can be combined while each has individual response rates and side effects. What is an optimal time efficient combined therapy stopping the spread while minimizing side effects? Since therapies can be combined, there is a two dimensional manifold in which therapy takes place. The strategy we suggest is to equip this manifold with a metric that allows us to find an effective combined therapy with minimal side effects. Effectiveness is defined by finding a path to a sufficiently low excitability where the tissue is not susceptible to spreading events, whereas efficiency refers to side effects and time.

I. Parameter space of the FHN system

We assume that a standard activator-inhibitor scheme leads to the observed propagation phenomena during SD. The activator and inhibitor variables, u and v, are coupled by their kinetic reaction rates $f(u,v)$ and $g(u,v)$, respectively, and can diffuse in the medium. The equations are

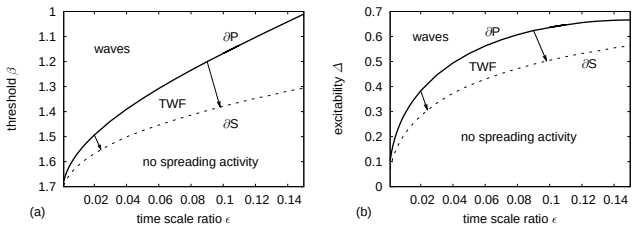

Fig. 2. Parameter space of the FHN system ($\gamma = 0, \delta = 0$). Besides the parameter ϵ, a *threshold parameter* β and an *excitability parameter* Δ is used in (a) and (b), respectively, to span the parameter space (see Fig. 1). Three regimes exist defined by the spatio-temporal patterns that occur: waves, transient wave forms (TWF) and no spreading activity. The arrows mark two paths which are perpendicular to the border ∂S in (a) but not in (b).

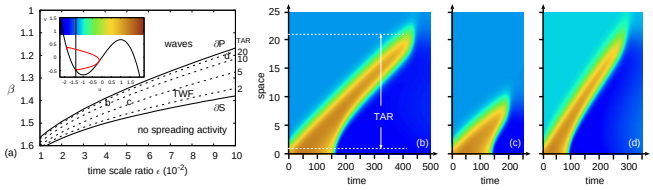

Fig. 3. (a) Parameter space with tissue-at-risk(TAR)-isolines (dashed). The extent a TWF spreads is defined from the stimulation border to the location where the maximum activator concentration u lies above the nullisocline $\dot{u} = 0$ (inset). The red curve in the inset is the projection of a TWF from the infinite phase space of the space-dependent FHN system into the one of the homogeneous system for $\beta = 1.4, \epsilon = 0.04$. The projection is taken at the moment which we defined as the collapse of the TWF. (b)-(d) Space-time plots of the transient wave forms (TWF) following a stimulation (increase of u by 2 for $0 < x < 1$, starting from the fixed point). Parameters: (b) $\epsilon = 0.04$, $\beta = 1.4$, (c) $\epsilon = 0.05, \beta = 1.4$, (d) $\epsilon = 0.095, \beta = 1.185$. $D_u = 1$ and $\delta = 0$ for all parts. The color code denotes the activator u as defined in the inset of panel (a).

$$\begin{aligned} \frac{\partial u}{\partial t} &= f(u,v) + D_u \frac{\partial^2 u}{\partial x^2} \\ \frac{\partial v}{\partial t} &= \epsilon g(u,v) + D_v \frac{\partial^2 v}{\partial x^2}. \end{aligned} \tag{1}$$

Diffusion is represented by diffusion coefficients D_u and D_v. By re-scaling space, the ratio $\delta = \frac{D_v}{D_u}$ of the diffusion coefficients can be introduced. The parameter ϵ is the time scale ratio of inhibitor and activator variables. The reaction rates $f(u,v)$ and $g(u,v)$ may possibly be derived from a more complex model of SD, e.g., the one from [20], by lumping together all activator variables, such as inward currents and extracellular potassium concentration $[K^+]_o$ into a single activator variable and their combined kinetics into a reaction rate $f(\cdot,\cdot)$. Likewise, a single inhibitor variable could be related to recovery processes, such as effective regulation of $[K^+]_o$ by the neuron's Na-K ion pump and the glia-endothelial system. This will be an important task of future investigations. We aim to describe universal features of reaction-diffusion coupling that lead to the onset of spreading pathological states and do not specify the variables u and v which underly these characteristics other than that they play the roles of activator and inhibitor, respectively. Their kinetic functions $f(u,v)$ and $g(u,v)$ are given by the FHN system

$$\begin{aligned} f(u,v) &= u - \frac{1}{3}u^3 - v \\ g(u,v) &= u + \beta - \gamma v \end{aligned} \tag{2}$$

where β and γ determine the excitation threshold (Fig. 1).

We shall start by viewing the parameter plane of the FHN model as a manifold M and consider its geometric structure. M has four dimensions $(\epsilon, \beta, \gamma, \delta)$. In a certain regime the parameters β and γ determine the threshold for a non-or-all excitation process. Like ϵ, their variation can cause a bifurcation: the emergence of sustained travelling waves. Instead of the four dimensions usually a two dimensional subset is investigated to describe this bifurcation, for example the section at $\gamma = 0.5$ [34], or at $\gamma = 0$ [35], both with

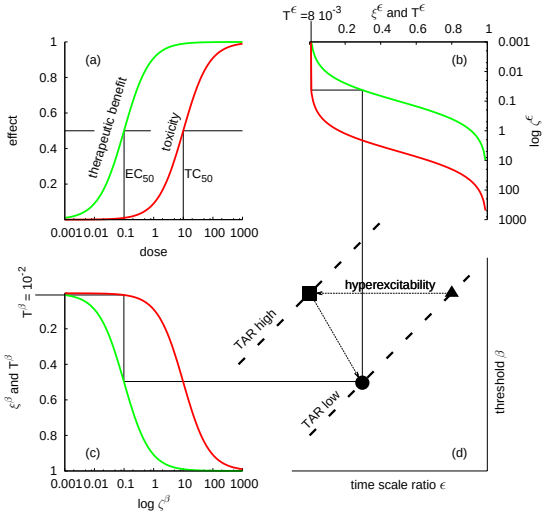

Fig. 4. (a) Dose response curves for an effective dose and a toxic dose with the typical sigmoidal shape caused by the logarithmic scaling. (b),(c) Same as in (a), but with rotated and inverted axes for two drugs ζ^ϵ acting on ϵ and ζ^β acting on β. (d) Schematic parameter space with two TAR-isolines (TAR high and TAR low). A route to hyperexcitability can be caused by a shift in ϵ (from ▲ to ■). The optimum path from the hyperexcitable state (■) towards the isoline of the physiological state (TAR low) using the two dose and toxic response curves in (b) and (c) leads to (●).

$\delta = 0$. Consider the subset at $\gamma = 0$. A particular FHN system is specified by a point q of this subset. It can be parameterized by the coordinate functions $\epsilon(q)$, i. e., the time scale separation of u and v, and the threshold parameters $\beta(q)$. As an alternative coordinate function for $\beta(q)$

$$\Delta(p) = (\beta - \frac{1}{3}\beta^3) \tag{3}$$

can be chosen [35]. While β is a measure of the threshold, Δ is related to a measure of excitability, because it is equal to the inhibitor concentration in the steady state (Fig. 1). This is rather a convention than a definition of excitability. To be more general, we shall only assume that excitability E is a C^∞-function $E : U \to \mathbb{R}$ in a subset U of M. Further properties of this function will be defined later. Firstly we want to note that there obviously exists a whole set of coordinate systems $\mathcal{A}$ for M with coordinate transformations like Eq. (3) being C^∞ diffeomorphisms. Naturally, M can be identified as a C^∞ differential manifold. For a given subset U of dimension n we can chose the coordinate system $\xi = [\xi^1, \ldots, \xi^n] = [\xi^i] \in \mathcal{A}$, with $i \in \{1, 2, \ldots, n\}$ that seems to suit best the purpose of study. Thus, in the section with $n=2$ and $\xi^1=\epsilon$ the parameter ξ^2 can be chosen either as β or as Δ. We will mainly consider the hypersection at $\delta = 0$, and $\gamma = 0$ unless explicitly stated otherwise, and use various coordinate systems in this submanifold.

II. Transient Wave Forms (TWF)

Excitability is an emergent property of active media. It arises when a critical parameter value is crossed above which the medium is susceptible for sustained propagating excitation patterns [37], [34], [35]. In a 1D medium this border in M is the propagation boundary ∂P. Below ∂P any confined perturbation of arbitrary profile decays eventually. Above ∂P some wave profiles are stable and travel with constant velocity. In a co-moving frame, these travelling waves are equivalent to the existence of a homoclinic orbit. The transition marks a bifurcation of codimension one. Therefore ∂P is a hypersurface in M separating the regime supporting travelling waves from the non-excitable one. In a two-dimensional parameter space, spanned by ϵ, and β or Δ, ∂P is a curve defined by fold points (Fig. 2). We consider the region *close* to ∂P, where TWF exist though sustained waves may not.

In the absence of a metric on M closeness to ∂P can be defined with reference to other borders by which M is further subdivided. The adjacent bifurcation curve above ∂P is ∂R, which is defined only in systems with more than one spatial dimension. In these systems ∂R is the border above which open wave fronts will not disappear because the open ends curl in to form a spiral shape. Open waves rotate and re-enter multiple times the invaded tissue. Between ∂R and ∂P TWF exist, depending on the initial size and shape. In this study, we will consider only one spatial dimension. Therefore we only investigate the region below ∂P, because above ∂P such TWF do only exist for spatial dimensions higher than one.

We suggest to take the distance a TWF spreads to define isolines in the regime below ∂P. This distance defines the volume of tissue at risk (TAR, see Fig. 3 (b)) referring to the risk of transient neurological symptoms or even of permanent damage (PID case) when this tissue is invaded following a local stimulation. We define a new boundary ∂S as TAR approaching 0. At ∂S any stimulation collapses into the steady state without affecting surrounding tissue. On the contrary, at ∂P the TAR is infinite, as stable waves exist which spread through the whole tissue. The region between ∂S and ∂P is the region where in a 1D system TWF exist. This region defines a subset U of M. The general point of a therapeutic control strategy is to leave U by crossing ∂S.

III. Efficient control of transient wave forms

So far excitability E has not been defined. We assume E to be a C^∞-function in U. In fact, it is reasonable to assume that E is constant on the two borders, because these are bifurcation lines at which TAR is constant. Furthermore, since a change in TAR is suggestive of a change in excitability, we propose both to be linearly related. Our goal is to control a path Λ in U along which excitability, and with it the volume of TAR, is efficiently diminished. Let the path Λ start in U at q where the neuronal tissue temporarily supports the spread of excitation. Let the path end on ∂S. Firstly, we assume sufficient knowledge of control characteristics, e. g., by pharmacokinetic and pharmacodynamic means, as described in the next section. We will show in the next section that this provides a metric on U. In this section we will just *assume* U to be a differential manifold with a metric. Furthermore, we assume (i) that our control method allows us to choose any path $\Lambda : I \to U$ parameterized by

some interval $I \subset \mathbb{R}$, (ii), as already stated, (ii) that E is a C^∞-function in a subset U, which includes Λ, and (iii) that $E(q) > E(\partial S)$ holds.

Which path should we take, if we want to reduce excitability by going from q to ∂S by deliberate control? The efficiency of successful control dragging the system into the target state p on ∂S should be given by some optimization criterion. When a metric is given two paths are privileged: the shortest path Λ_s between q and ∂S, and also the one that minimizes E by gradient descent. The latter path Λ_g implies a metric because covectors like $\partial E/\partial \xi^j$ and tangent vectors to a path Λ are unrelated objects of different kinds. Only a metric tensor g_{ij} defines the gradient as a contravariant vector (using summation convention)

$$(\text{grad}E)^i = g^{ij}\frac{\partial E}{\partial \xi^j}. \tag{4}$$

Therefore, only when a metric is given on U, we can apply some optimization criterion for the therapeutic path.

IV. Metric tensor on U

As efficient control, in the last section we proposed a method based on a metric structure in U. Therefore, a metric structure is needed to optimize control. Hence it is natural in this context to endow U with a metric that is derived by some sort of cost function of the control method. We introduce a standard pharmacokinetic and pharmacodynamic scheme to illustrate this concept. Let ζ^i be the concentrations of drugs which regulate diverse functions in populations of neurons. For the sake of simplicity, we neglect the details of pharmacokinetics as the discipline that describes dosage regimes and the time-course of ζ^i in the body by absorption, distribution, metabolism, and excretation. We assume the drugs can be constantly administered and their rate of administrations equals their rate of metabolism and excretion. Thus ζ^i is immediately in its steady state value. Furthermore, we assume that ζ^i follows linear pharmacokinetics. In this situation the steady state of ζ^i changes proportionally according to dose.

The relation between drug dose and response is usually modeled as a hyperbolic function assuming a simple drug receptor interaction. Suppose the response to ζ^i is a displacement in U given without loss of generality in the coordinate system $\xi = [\xi^1, \ldots, \xi^n]$

$$\xi^i = r^i\left(\frac{\xi^i_{max}\zeta^i}{EC^i_{50} + \zeta^i}\right). \tag{5}$$

In this equation, r^i denotes transducer functions that represent the response of the FHN system to the drug ζ^i. For the sake of simplicity we use as transducer functions r^i the identity. EC^i_{50} are the *effective doses 50*, i.e., doses at which 50% of the maximal responses ξ^i_{max} are achieved. ξ^i_{max} is the asymptotic value of ξ^i for large concentrations.

In analogy with Eq. (3), where we have introduced the new coordinate Δ, we have thus introduced the coordinate system $\zeta \in \mathcal{A}$ as new control parameters of the FHN system. Although the coordinate system ζ is a privileged reference system for U by selecting ζ^i, we can not simply assume it to be Cartesian. Note, that commonly the logarithm of the concentration ζ^i is plotted on the abscissa (Fig. 4 (a)). Thus, the choice of the unit of concentration is arbitrary.

Let us write the components of the metric tensor of U in the coordinate system ζ as g_{ij}. We can introduce a new coordinate system $\xi \in \mathcal{A}$ of the response variables. The components of the metric tensor in this coordinate system ξ are

$$\tilde{g}_{\alpha\beta} = \frac{\partial \zeta^i}{\partial \xi^\alpha} g_{ij} \frac{\partial \zeta^j}{\partial \xi^\beta}. \tag{6}$$

Likewise, we can calculate the components g_{ij} from $\tilde{g}_{ij}$. Hence the question is whether a structure of the pharmacodynamic scheme can be treated as a metric structure in differential geometry defining $\tilde{g}_{ij}$. Suppose that ζ^i or one of their metabolites have toxic side effects. Their dose response curve follows the same relation as Eq. (5), although shifted to the right on the dose axis by a higher *toxic dose 50* (TC_{50})

$$T^i = t^i\left(\frac{T^i_{max}\zeta^i}{TC^i_{50} + \zeta^i}\right). \tag{7}$$

t^i denotes transducer functions that represent the response of the toxic system. Again for the sake of simplicity we use as transducer functions t^i the identity function. In analogy to Eq. (6) we obtain

$$\tilde{g}_{\alpha\beta} = \frac{\partial \zeta^i}{\partial \xi^\alpha}\frac{\partial T^k}{\partial \zeta^i}\delta_{kl}\frac{\partial T^l}{\partial \zeta^j}\frac{\partial \zeta^j}{\partial \xi^\beta}, \tag{8}$$

assuming $[T^1, \ldots, T^n]$ builds a Cartesian coordinate system of the costs with the Euclidean metric δ_{kl}.

We end this section with one example corresponding to a subtype of migraine with aura for which pathogenic genetic mutations are known. A recent study by [38] showed that a novel migraine mutation introduced in the gene coding the sodium channel leads to a slowed-down inactivation and a two-fold faster recovery from inactivation. Thus the physiological state of the cortex is shifted into hyperexcitability in our simplified FHN model by slowed inhibition, i. e., lower ϵ values. Now suppose that we have a drug with concentration ζ^1 acting exclusively on ϵ (e. g., $\xi^1 \equiv \epsilon$) and another ζ^2 acting exclusively on β (e. g., $\xi^2 \equiv \beta$). For the sake of readability we replace the set $\{1, 2\}$ of indices i by $\{\epsilon, \beta\}$ and use ζ^i for both the drug concentration and the drug name. Let the effective doses 50 EC^i_{50} be the same for both (without loss of generality we choose $EC^i_{50} = 0.1$), and let the toxic doses 50 TC^i_{50} differ. Usually TC^i_{50} is several times higher then the effective dose. We choose $TC^\epsilon_{50} = 5$ and $TC^\beta_{50} = 10$. The drug ζ^β has therefore a relatively higher therapeutic index $TI^i = TC^i_{50}/EC^i_{50}$ than ζ^ϵ (Fig. 4).

We now consider how the two drugs must be administered in a combined therapy. First, we assume that both drugs have a sufficient efficacy, that is, they are each potent enough to drag the FHN system back to it physiological excitability defined by the TAR-isoline (Fig. 4 d). The maximal response ξ^i_{max} rates for both are chosen such that already 80% of

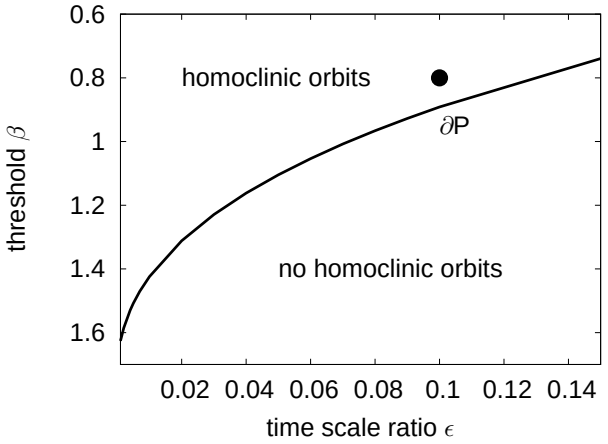

Fig. 5. Parameter space of the FHN system at the section $\gamma = 0.5$. ∂P is the propagation boundary. Below ∂P any confined perturbation of arbitrary profile decays eventually. Above ∂P some wave profiles are stable and propagate with constant speed. They correspond to homoclinic orbits in a co-moving frame. The simulations have been done with a FHN system at $\beta = 0.8$ and $\epsilon = 0.1$ (solid black circle). A successful suppression of reaction-diffusion waves by nonlocal coupling indicates a shift of ∂P of the combined system beyond the point at $\beta = 0.8$ and $\epsilon = 0.1$.

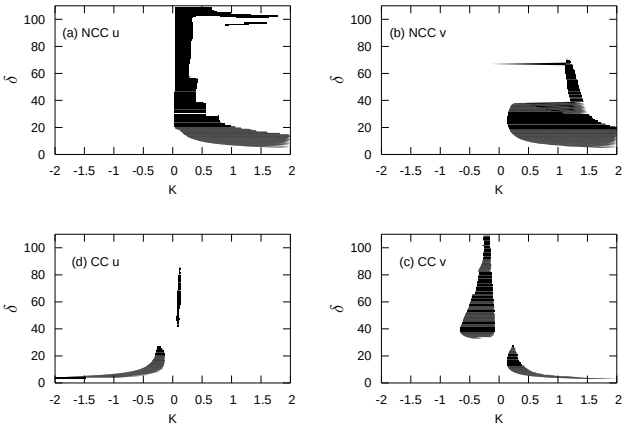

Fig. 6. Parameter plane (K, δ) of the nonlocal control term. Black areas indicate successful suppression of wave propagation. (a) Non-cross coupling (NCC) in the activator equation (9). (b) NCC in the inhibitor equation (10). (c) Cross coupling (CC) in the activator equation (9). (d) CC in the inhibitor equation (10).

ξ^i_{max} is effective. Without loss of generality we fix T^i_{max} at ξ^i_{max}. If only ζ^ϵ is available, the physiological TAR level is crossed at 7.4% of the maximal toxic level of T^ϵ. A pure administration of neuromodulator ζ^β with doubled and halved therapeutic index TI^ϵ cost 3.85% of the maximal toxic level T^β. An optimal combined therapy with therapeutic index TI^β reaches the physiological TAR level at 1.84% of the maximal combined toxic level $T_{tot} = T^\epsilon + T^\beta$ (see the two black lines terminating at the effect axes in Fig. 4).

V. Suppression of waves by nonlocal interaction

Psychophysical studies on visual processing in migraine patients suggest that changes in their networks of cortical neurons lead to an interictal state of changed excitability, i. e., an anomalous cortical state in the interval between migraine attacks [39], [40]. This motivates efforts to understand how the spread of reaction diffusion waves is controlled by nonlocal network connectivity.

To investigate the influence of various nonlocal connectivity schemes on wave propagation in the regime of sub-excitability, we start by setting a super-threshold stimulation in the one-dimensional system, choosing a particular FHN system with parameter values $\beta = 0.8$, $\epsilon = 0.1$, $\gamma = 0.5$, $D_u = 1$, and $D_v = 0$. Once a stable one-dimensional wave profile is obtained, a nonlocal lateral network is switched on

$$\begin{aligned} \frac{\partial u}{\partial t} &= u - \frac{1}{3}u^3 - v + \frac{\partial^2 u}{\partial x^2} \\ &\quad + \text{nonlocal coupling} \qquad (9) \\ \frac{\partial v}{\partial t} &= \epsilon(u + \beta - \gamma v) \\ &\quad + \text{nonlocal coupling} \, . \qquad (10) \end{aligned}$$

The nonlocal coupling terms have the form

$$K\left[s(x+\delta) - 2s(x) + s(x-\delta)\right] . \qquad (11)$$

The signal s can either be the activator u or inhibitor v. A connection in the cortex can extend over several millimeters and it either mediates competitive or cooperative interactions. The parameter δ describes the connection length and the coupling strength K of the interaction.

Different networks for various parameter values K and δ are classified by their effect on the wave. We distinguish two cases. Either the wave is suppressed. This indicates that the excitability boundary ∂P of the combined system is shifted to higher excitability values (upwards in Fig. 5) into a regime where without the nonlocal coupling pulse solutions would exit. Or the wave continues to spread, though its profile and speed might change. From a clinical point of view, the wave suppression is a desirable control goal for the network achieved within the solid black regions in the (K, δ)-planes in Fig. 6.

We find that wave propagation can be suppressed with a NCC (non-cross-coupled) setup only with positive coupling strength K. When the NCC term appears in the activator balance equation, the desired control goal is achieved largely independent of the connection length δ (Fig. 6 a), as long as δ is in the range of the wave width, including its refractory tail. When the nonlocal coupling term appears in the inhibitor balance equation, a similar picture arises, though waves are suppressed for connection lengths ranging into the refractory tail of the wave ($\delta > 40$) only for a narrow regime of K. Suppression completely fails for $\delta > 70$ (Fig. 6 b).

Cross coupling of inhibitor and activator achieves the desired control goal for both positive and negative coupling strengths K, depending on the connection length δ (Fig. 6 c-d). The area in the parameter plane (δ, K) where this control goal is achieved resembles a Mexican-hat-type network connectivity. This is readily seen in Fig. 7. When the nonlocal term appears in the inhibitor balance equation (10) the regimes of successful control in the K direction is much wider (Fig. 6 d) than the regime for cross coupling in the

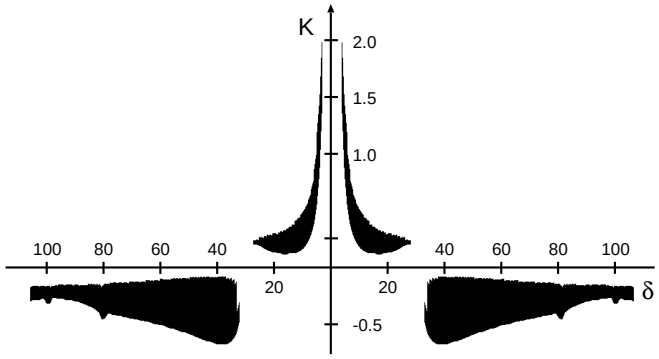

Fig. 7. The "Mexican hat" connectivity profile of successful wave suppression for cross coupling (CC) is clearly visible when the control plane is rotated and the space coordinate δ is plotted as the distance ranging from negative to positive values. Shown is the successful control area (black) for the CC term appearing in the inhibitor equation (10). When the CC term is in the activator equation (9) the profile of the Mexican-hat connectivity is inverted.

activator balance equation (9, Fig. 6 c).

VI. Discussion

The phenotypical scheme of spreading depression describes transient waves of massive depolarization of neurons and astrocytes. Such *spreading depolarization* [15] is associated with migraine, epilepsy and stroke. Their etiologies are mainly discussed in the context of hyperexcitability and disorders known as channelopathies, that is, diseases caused by a mutation in gene coding for ion channels. The challenge is to bridge the gap between the molecular level of the cause and macroscopic *tissue* level of the effects.

We suggest that there are at least two independed routes towards a hyperexcitable state that supports transient wave forms in cortical tissue: one changing the ratio of kinetic rates ϵ and one lowering the threshold β. While the latter route changes the nullclines, the former changes only the trajectories in the phase space. Consequently, there are also two routes out of the hyperexcitable regime. This is of particular interest when a critical therapeutic time window exits in which the volume of affected tissue is largely increased, as for example in peri-infarct depolarization. Then the therapeutic aim would be first to prevent tissue loss within the given window and re-establish the physiological value later. In Fig. 4 (d) this would correspond to a path from the hyperexcitable state (■) directly to a state of low tissue at risk (●) and from there back to the physiological state (▲).

We have described efficient control of excitability by a simple pharmacodynamic model. In general, the study of beneficial effects of independent pathways is complicated by numerous interactions between pharmacokinetics, pharmacodynamics, and homeostatic factors and by individual variability. For example, the introduction of antagonistic behavior between ζ^ϵ and ζ^β will complicate the geometrical structure of U. In general the coordinate system of the costs $[T^1, \ldots, T^n]$ will not build a Cartesian coordinate system. However, if we have a mapping from general costs and effects defined by Eqs. (5) and (7) we still can infer a metric structure of the parameter space of FHN. This may even lead to a general definition of excitability.

Furthermore, we showed that certain control schemes of an inhibitor-activator type system shift the emergence of wave propagation towards higher values of excitability. The control we investigated is of the form of a nonlocal coupling given in Eq. (11). This nonlocal transaction was added to the reaction-diffusion mechansim either in the inhibitor or the activator balance equation. The sum of all individual cross coupling terms that achieve a clinically desirable control goal takes the shape of an upright or inverted Mexican hat, respectively. This supports our assumption that the nonlocal coupling results from intrinsic lateral cortical connections. Dichotomic lateral interaction is an architecture widely used in models of topographic feature maps.

To summarize, in modeling migraine a major objective is to understanding cortical susceptibility to focal neurological symptoms in terms of neural circuitry [42], [43], [**?**]. This could open up to us new strategies for therapy using methods of controlling complex dynamics. Control of complex dynamics has evolved during the last decade as one of the central issues in applied nonlinear science [44]. Progress toward clinical implementation of nonlinear methods has been done so far in neurology in particular in Parkinson's disease, a neurological diseases also characterized by pathological brain synchrony. There, techniques based on control of complex dynamics [45] are now tested in clinical studies and fundamentally novel therapy methods are being evolved [46]. It is hoped that this success can be expanded.

References

[1] M. Lauritzen, "Pathophysiology of the migraine aura. the spreading depression theory [see comments]," *Brain*, vol. 117, pp. 199–210, 1994.

[2] S. K. Aurora, B. K. Ahmad, K. M. Welch, P. Bhardhwaj, and N. M. Ramadan, "Transcranial magnetic stimulation confirms hyperexcitability of occipital cortex in migraine," *Neurology*, vol. 50, pp. 1111–1114, 1998.

[3] K. M. Welch, "Brain hyperexcitability: the basis for antiepileptic drugs in migraine prevention," *Headache*, vol. 45, pp. 25–32, 2005.

[4] K. Lashley, "Patterns of cerebral integration inicated by scotomas of migraine," *Arch. Neurol. Psychiatry*, vol. 46, pp. 331–339, 1941.

[5] N. Hadjikhani, M. Sanchez Del. Rio., O. Wu, D. Schwartz, D. Bakker, B. Fischl, K. K. Kwong, F. M. Cutrer, B. R. Rosen, R. B. Tootell, A. G. Sorensen, and M. A. Moskowitz, "Mechanisms of migraine aura revealed by functional MRI in human visual cortex," *Proc. Natl. Acad. Sci. USA*, vol. 98, pp. 4687–4692, 2001.

[6] G. G. Somjen and P. G. Aitken, "The ionic and metabolic responses associated with neuronal depression of Leao's type in cerebral cortex and in hippocampal formation," *An. Acad. Bras. Cienc.*, vol. 56, no. 4, pp. 495–504, 1984.

[7] F. S. Giorgi, G. Lazzeri, G. Natale, A. Iudice, S. Ruggieri, A. Paparelli, L. Murri, and F. Fornai, "MDMA and seizures: a dangerous liaison?" *Ann. N. Y. Acad. Sci.*, vol. 1074, pp. 357–364, 2006.

[8] K. A. Schindler, H. Leung, K. Lehnertz, and C. E. Elger, "How generalized are secondarily "generalized" tonic-clonic seizures?" *J Neurol Neurosurg Psychiatry*, 2007.

[9] M. Nedergaard and J. Astrup, "Infarct rim: effect of hyperglycemia on direct current potential and [14C]2-deoxyglucose phosphorylation," *J. Cereb. Blood Flow Metab.*, vol. 6, pp. 607–615, 1986.

[10] K. A. Hossmann, "Viability thresholds and the penumbra of focal ischemia," *Ann. Neurol.*, vol. 36, pp. 557–565, 1994.

[11] M. Fisher and K. Takano, "The penumbra, therapeutic time window and acute ischaemic stroke," *Baillieres Clin. Neurol.*, vol. 4, pp. 279–295, 1995.

[12] A. E. Baird, A. Benfield, G. Schlaug, B. Siewert, K. O. Lovblad, R. R. Edelman, and S. Warach, "Enlargement of human cerebral ischemic lesion volumes measured by diffusion-weighted magnetic resonance imaging," *Ann. Neurol.*, vol. 41, pp. 581–589, 1997.

[13] A. M. Hakim, "Ischemic penumbra: the therapeutic window," *Neurology*, vol. 51, no. 3 Suppl 3, pp. 44–46, 1998.

[14] T. Back, "Pathophysiology of the ischemic penumbra–revision of a concept," *Cell. Mol. Neurobiol.*, vol. 18, pp. 621–638, 1998.

[15] J. P. Dreier, J. Woitzik, M. Fabricius, R. Bhatia, S. Major, C. Drenckhahn, T.-N. Lehmann, A. Sarrafzadeh, L. Willumsen, J. A. Hartings, O. W. Sakowitz, J. H. Seemann, A. Thieme, M. Lauritzen, and A. J. Strong, "Delayed ischaemic neurological deficits after subarachnoid haemorrhage are associated with clusters of spreading depolarizations," *Brain*, vol. 129, pp. 3224–3237, 2006.

[16] A. A. P. Leão, "Spreading depression of activity in the cerebral cortex," *J. Neurophysiol.*, vol. 7, pp. 359–390, 1944.

[17] A. Mayevsky, A. Doron, T. Manor, S. Meilin, N. Zarchin, and G. E. Ouaknine, "Cortical spreading depression recorded from the human brain using a multiparametric monitoring system," *Brain Res.*, vol. 740, pp. 268–274, 1996.

[18] C. Strümpel, Y. A. Astrov, and H. G. Purwins., "Multioscillatory patterns in a hybrid semiconductor gas-discharge system." *Phys. Rev. E*, vol. 65, p. 066210, 2002.

[19] M. Fabricius, S. Fuhr, R. Bhatia, M. Boutelle, P. Hashemi, A. J. Strong, and M. Lauritzen, "Cortical spreading depression and peri-infarct depolarization in acutely injured human cerebral cortex," *Brain*, vol. 129, pp. 778–790, 2006.

[20] H. Kager, W. J. Wadman, and G. G. Somjen, "Simulated seizures and spreading depression in a neuron model incorporating interstitial space and ion concentrations," *J. Neurophysiol.*, vol. 84, pp. 495–512, 2000.

[21] J. Bureš, O. Burešova, and J. Křivánek, *The mechanism and applications of Leão's Spreading Depression*. New York: Academia, 1974.

[22] A. Gorji and E.-J. Speckmann, "Spreading depression enhances the spontaneous epileptiform activity in human neocortical tissues," *Eur. J. Neurosci.*, vol. 19, pp. 3371–3374, 2004.

[23] G. G. Somjen, "Mechanisms of spreading depression and hypoxic spreading depression-like depolarization," *Physiol. Rev.*, vol. 81, pp. 1065–1096, 2001.

[24] C. Tobiasz and C. Nicholson, "Tetrodotoxin resistant propagation and extracellular sodium changes during spreading depression in rat cerebellum," *Brain Res.*, vol. 241, pp. 329–333, 1982.

[25] H. Martins-Ferreira, M. Nedergaard, and C. Nicholson, "Perspectives on spreading depression," *Brain. Res. Brain Res. Rev.*, vol. 32, no. 1, pp. 215–234, 2000.

[26] M. A. Dahlem and E. P. Chronicle, "A computational perspective on migraine aura," *Prog. Neurobiol.*, vol. 74, no. 6, pp. 351–361, 2004.

[27] H. C. Tuckwell and M. R. M., "A mathematical model for spreading cortical depression," *Biophysical J.*, vol. 23, pp. 257–276, 1978.

[28] J. A. Reggia and D. Montgomery, "Modeling cortical spreading depression," *Proc. Annu. Symp. Comput. Appl. Med. Care*, pp. 873–877, 1994.

[29] B. E. Shapiro, "Osmotic forces and gap junctions in spreading depression: a computational model," *J. Comput. Neurosci.*, vol. 10, pp. 99–120, 2001.

[30] A. L. Hodgkin and A. F. Huxley, "A quantitative description of membrane current and its application to conduction and excitation in nerve," *J. Physiol.*, vol. 117, p. 500, 1952.

[31] R. FitzHugh, "Impulses and physiological states in theoretical models of nerve membrane," *Biophys. J.*, vol. 1, pp. 445–466, 1961.

[32] J. Nagumo, S. Arimoto, and S. Yoshizawa., "An active pulse transmission line simulating nerve axon." *Proc. IRE*, vol. 50, p. 2061, 1962.

[33] M. A. Dahlem and S. C. Müller, "Reaction-diffusion waves in neuronal tissue and the window of cortical excitability," *Ann. Phys.*, vol. 13, no. 7, pp. 442–449, 2004.

[34] A. T. Winfree, "Varieties of spiral wave behaviour: An experimentalist's approach to the theory of excitable media," *Chaos*, vol. 1, pp. 303–334, 1991.

[35] V. Hakim and A. Karma, "Theory of spiral wave dynamics in weakly excitable media: asymptotic reduction to a kinematic model and applications," *Phys. Rev. E*, vol. 60, pp. 5073–5105, 1999.

[36] A. S. Mikhailov and K. Showalter, "Control of waves, patterns and turbulence in chemical systems," *Phys. Rep.*, vol. 425, pp. 79–194, 2006.

[37] A. S. Mikhailov and V. S. Zykov, "Kinematical theory of spiral waves in excitable media: comparison with numerical simulations," *Physica D*, vol. 52, pp. 379–397, 1991.

[38] K. R. J. Vanmolkot, E. Babini, B. de Vries, A. H. Stam, T. Freilinger, G. M. Terwindt, L. Norris, J. Haan, R. R. Frants, N. M. Ramadan, M. D. Ferrari, M. Pusch, A. M. J. M. van den Maagdenberg, and M. Dichgans, "The novel p.L1649Q mutation in the SCN1A epilepsy gene is associated with familial hemiplegic migraine: genetic and functional studies." *Hum. Mutat.*, vol. 28, p. 522, 2007.

[39] K. M. Welch, G. D'Andrea, N. Tepley, G. Barkley, and N. M. Ramadan, "The concept of migraine as a state of central neuronal hyperexcitability," *Neurol Clin*, vol. 8, no. 4, pp. 817–828, 1990.

[40] A. J. Shepherd, "Increased visual after-effects following pattern adaptation in migraine: a lack of intracortical excitation?" *Brain*, vol. 124, pp. 2310–2318, 2001.

[41] M. A. Dahlem, F. M. Schneider, and E. Schöll, "Efficient control of transient wave forms to prevent spreading depolarizations," *submitted to J. Theo. Biol.*, 2007.

[42] L. H. A. Monteiro, D. C. Paiva, and J. R. C. Piqueira, "Spreading depression in mainly locally connected cellular automaton," *J. of Biol. Systems*, vol. 14, pp. 617–629, 2006.

[43] E. Schöll and H. G. Schuster, Eds., *Handbook of Chaos Control*. Weinheim: Wiley-VCH, 2007, second completely revised and enlarged edition.

[44] P. A. Tass, J. Klosterkotter, F. Schneider, D. Lenartz, A. Koulousakis, and V. Sturm, "Obsessive-compulsive disorder: development of demand-controlled deep brain stimulation with methods from stochastic phase resetting," *Neuropsychopharmacology*, vol. 28 Suppl 1, pp. 27–34, 2003.

[45] C. Hauptmann and P. A. Tass, "Therapeutic rewiring by means of desynchronizing brain stimulation," *Biosystems*, vol. 89, pp. 173–181, 2007.